

NUMERICAL SYNTHESIS OF IONOGRAMS IN HORIZONTALLY INHOMOGENEOUS IONOSPHERE ON THE BASIS OF COMPOUND PARABOLIC LAYER MODEL

O.A. Laryunin

*Institute of Solar-Terrestrial Physics SB RAS, Irkutsk, Russia,
laroleg@inbox.ru*

Characteristic U-shaped traces (cusps) on ionograms have been identified as off-angle echoes from sloping electron density contours caused by the presence of traveling ionospheric disturbances (TIDs). Temporal evolution of the cusps is associated with horizontal drift of the disturbances.

A potential for reducing calculation time in numerical synthesis of vertical ionograms is under discussion.

Since numerical ray tracing is computationally intensive, we have developed simplified formulation for this study. The suggested model of compound parabolic layer allows us to analytically calculate ray paths. Changes in the shape of the ionogram cusp caused by varying TID characteristics are examined.

Keywords Ionosphere · Vertical sounding · Ionogram

INTRODUCTION

Vertical and near-vertical ionograms often show an additional U-shaped trace, which is called cusp and indicates the presence of a traveling ionospheric disturbance (TID) (Figure 1).

The cusp usually progresses toward lower frequencies and smaller group delays (downward along the ionogram trace), merging with the main trace of the ionogram [Danilkin et al., 1987; Krasheninnikov, Lyannoi, 1991]. As early as the last mid-century, it was shown [Munro, Heisler, 1956] that U-shaped traces appear on ionograms due to TIDs, which give rise to horizontal electron density gradients in the ionosphere and thus to off-angle reflections in radio sounding.

So-called satellite traces on ionograms (Figure 2 that illustrates vertical ionospheric sounding) have been examined in [Lynn et al., 2013]. The authors also associate this phenomenon with off-vertical echoes from moving electron density gradients. They give a consistent explanation on the basis of the model of tilted ionospheric reflector.

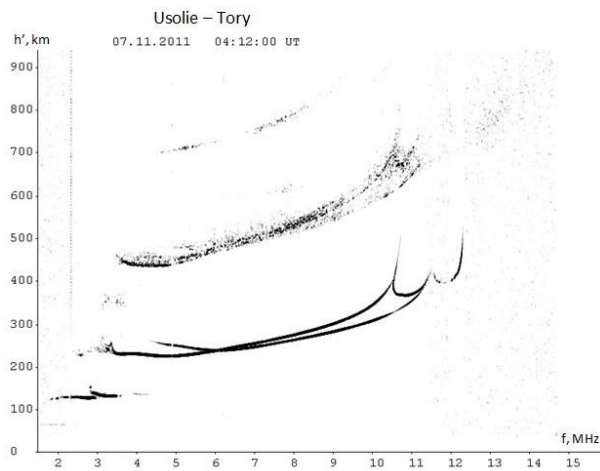
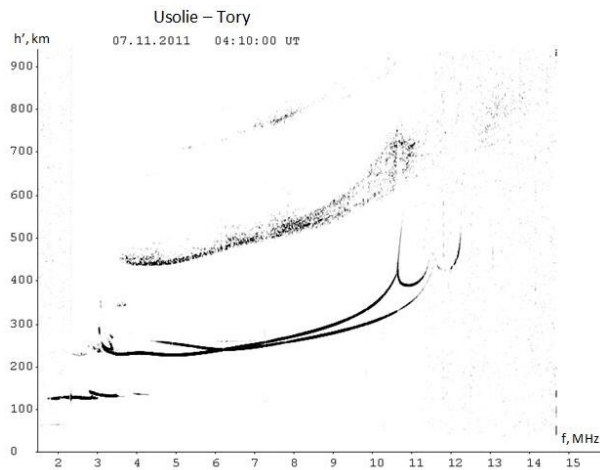
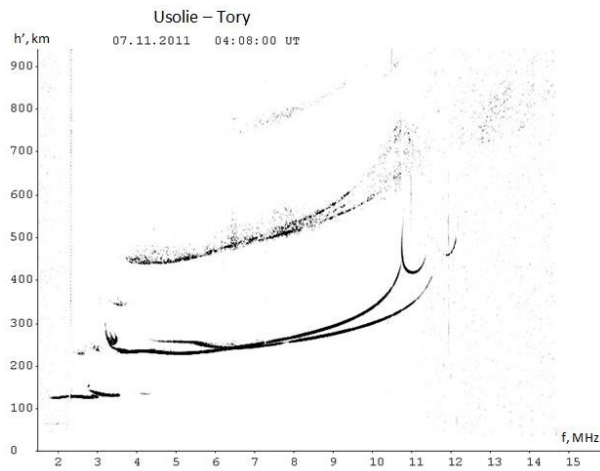
The numerical simulation in the present study uses a geometrical optics (GO) method, ignoring effects of Earth's magnetic field. The method is based on an assumption about insignificant change of the refractive index at a distance of one wavelength. This assumption is generally fulfilled in the ionosphere. The GO method exploits the concept of ray paths along which energy fluxes propagate. Ray paths are calculated by integrating ray equations (see below). In this case, the singularity at the point of reflection is integrable.

The horizontal gradient of ionization can be specified by different models, which give no significant differences when synthesizing a cusp. In particular, the following models are considered reasonable.

1. The model of sinusoidal perturbation (here the passage of a cusp on the ionogram corresponds to one TID period [Munro, Heisler, 1956]):

$$N(z, x, t) = N_0(z) (1 + \delta \cos(k_z z + k_x x - (2\pi/T)t + \Phi_0)), \quad (1)$$

where N is the electron density as a function of coordinates and time; δ is the TID amplitude; $k_x = (2\pi/\Lambda) \sin \gamma$, $k_z = (2\pi/\Lambda) \cos \gamma$ are components of the TID wave vector with the wavelength Λ ; T is the TID period; Φ_0 is the initial phase; the angle γ specifies the direction of phase velocity of the disturbance.



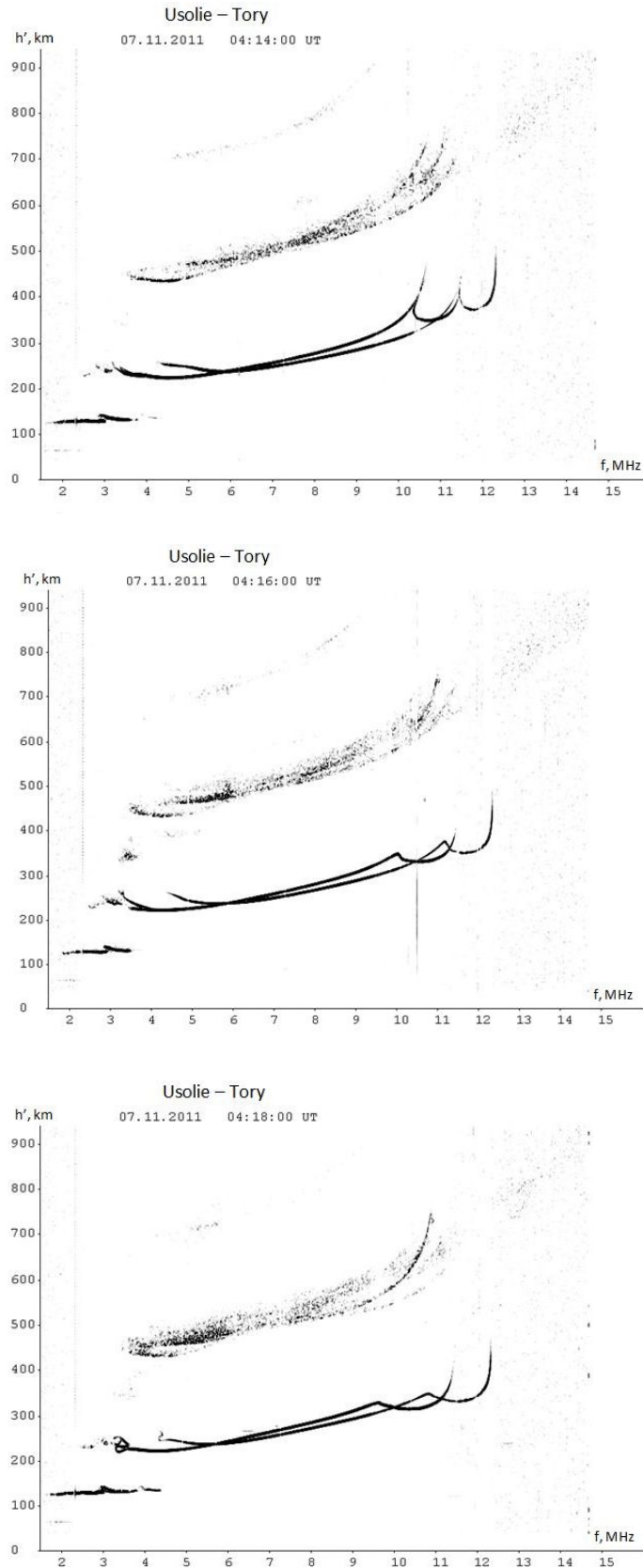


Figure 1. Cusp evolution on near-vertical ionograms for November 7, 2011 The data are presented with a 2 min interval. The ground range is 120 km

2. The model of tilted layer representing Gaussian enhancement in the background ionosphere (Figure 3, a):

$$N(x, z) = N_0(z) \left[1 + \delta \times \exp \left[- \left(\frac{(z - z_0) \cos \psi + (x - x_0) \sin \psi}{z_b} \right)^2 - \left(\frac{(x - x_0) \cos \psi + (z - z_0) \sin \psi}{x_b} \right)^2 \right] \right], \quad (2)$$

where $N_0(z)$ is the background electron density profile; ψ is the tilt of the disturbance; x_0, z_0 are coordinates of any point in the maximum of the disturbance ($z_0 = a + x_0 \tan \psi$, where a is the arbitrary parameter); z_b is the scale of the disturbance; $x_b \gg z_b$.

For example, Laryunin et al. [Laryunin et al., 2014] point out that results of the simulation based on Expression (2) are in good agreement with experimental data. The authors also consider the possibilities of fitting the parameters of Model (2) to the experimental ionograms.

DESCRIPTION OF THE MODEL

Ray tracing in conditions of nonstratified ionosphere requires us to “home-in” on the given ground range, which is resource-intensive: to find one point of an ionogram, we must calculate a ray fan in a given range of angles with a sufficiently small step.

Thus, the fitting that boils down to the selection of four parameters δ, x_0, ψ , and z_b even for the relatively simple model of type (2) may be fraught with calculation difficulties.

In this regard, we suggest a simplified formulation for this study in order to reveal basic characteristics determining the dependence of the shape of the cusp on the parameters of nonstratified ionosphere. To reduce the computation time of ray tracing, I take advantage of the fact that 2D ray paths can be obtained analytically for model of parabolic ionospheric layer (3) if effects of Earth’s magnetic field are neglected (see Appendix 1) [Eremenko et al., 2007];

$$f_p^2(z) = f_c^2 \left[1 - \left(\frac{z - z_m}{y_m} \right)^2 \right], \quad (3)$$

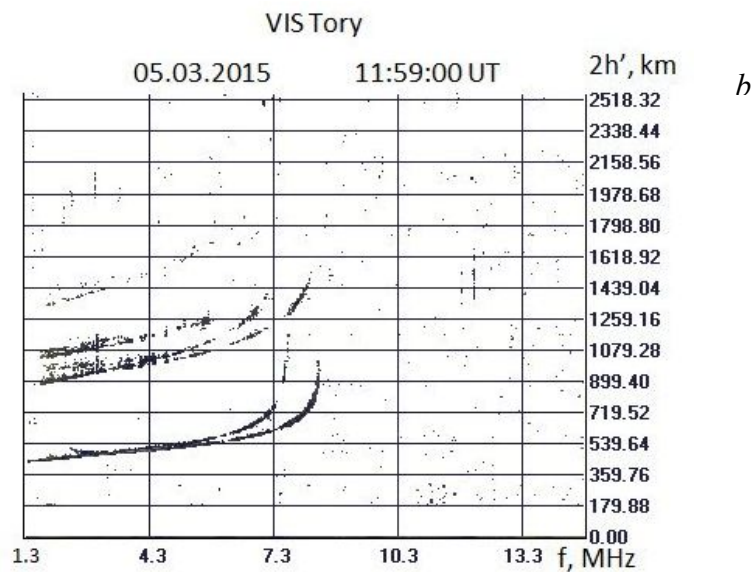
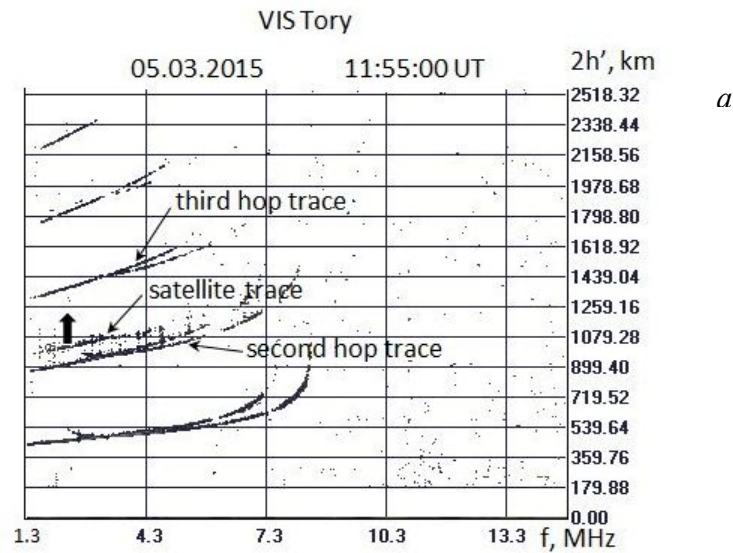
where z is the vertical coordinate, f_c is the critical frequency, z_m is the peak height of the layer, y_m is the semi-thickness of the layer.

Figure 4, a illustrates the implementation of the model of compound parabolic layer. Up-going (from the transmitter to the reflection point) and down-going (from the reflection point to the receiver) paths are identical and merge in the figure. Thick lines show characteristic homed-in ray paths corresponding to two different operating frequencies. The dashed line divides the ionosphere into two parts. The area below the line is background parabolic layer (3). Finding the point A (or B) reduces to the numerical solution of the transcendental equation $z_1(x) = z_2(x)$, where

$$z_1(x) = A_1 \exp\left(\frac{\Omega x}{\cos \varphi_0}\right) + A_2 \exp\left(-\frac{\Omega x}{\cos \varphi_0}\right) + z_m, \quad (4a)$$

$$z_2(x) = z_0 - x \operatorname{tg} \psi. \quad (4b)$$

Expression (4a) specifies the ray path in the area below the dashed line; the constants A_1 , A_2 , and Ω are determined by parameters of parabolic layer (3) and by the operating frequency (see Appendix 1). Expression (4b) specifies the boundary between the background layer and the attached tilted one. The parameters z_0 and ψ determine the position and slope of the dashed line, which serves as a notional boundary of the ionospheric disturbance. Then, in the simulation, a decrease in the parameter z_0 with time, i.e. descent of the attached tilted layer (which is equivalent to its leftward drift (Figure 4, a)), causes the cusp to descend downward, and the tilt ψ determines the shape of the cusp.



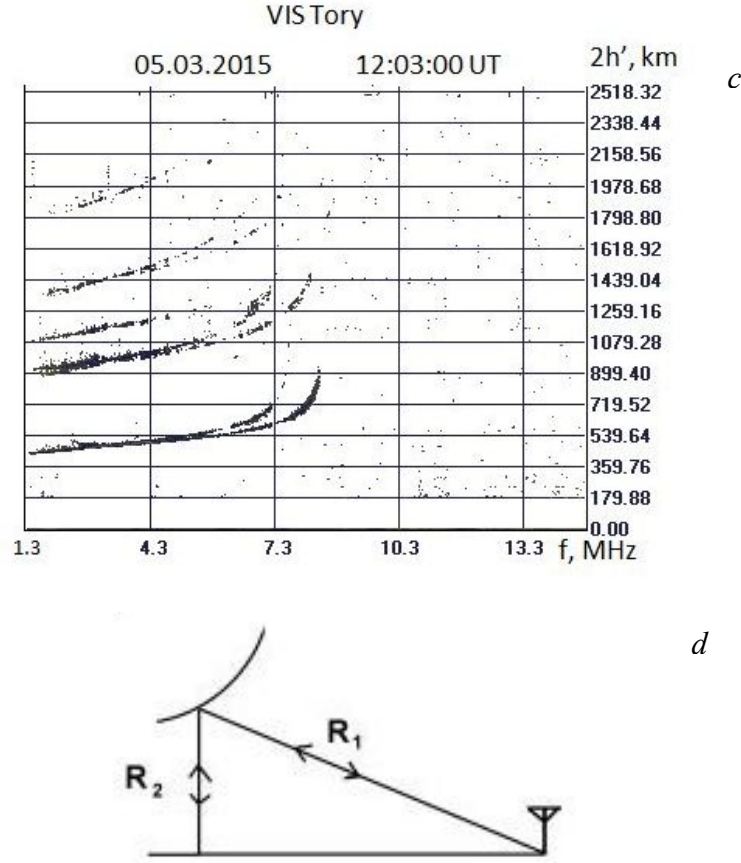


Figure 2. Temporal evolution of satellite trace on the ionograms (a–c); schematic representation of the respective TID (from [Lynn et al., 2013]) (d)

In this case, to home-in to zero distance, we search initial launch angles ϕ_0 to provide the 90° intersection of the paths with the dashed line.

Let us assume that rays entering perpendicularly the area above the dashed line propagate further rectilinearly along the Z' axis (Figure 4, a, path segments AP and BQ) in a new attached parabolic layer that imitates the profile in Figure 3. The maximum plasma frequency in the attached tilted layer is higher than the background one by a relative magnitude δ ; here the background plasma frequency is the value at the point where the rays (A or B, Figure 4, a) enter the layer.

For example, if the plasma frequency at the point A is $f_p(z_A)$, then rays AP and BQ propagate in parabolic layers of the form

$$f_{p1}^2(z') = f_{c1}^2 \left[1 - \left(\frac{z' - z'_m}{y'_m} \right)^2 \right], \tag{5}$$

where $f_{c1} = f_p(z_A)(1 + \delta)$ for AP and accordingly $f_{c1} = f_p(z_B)(1 + \delta)$ for BQ.

Since $f_p(z_A) \neq f_p(z_B)$, the critical frequency f_{c1} of the attached tilted layer depends on the point at which the ray enters it.

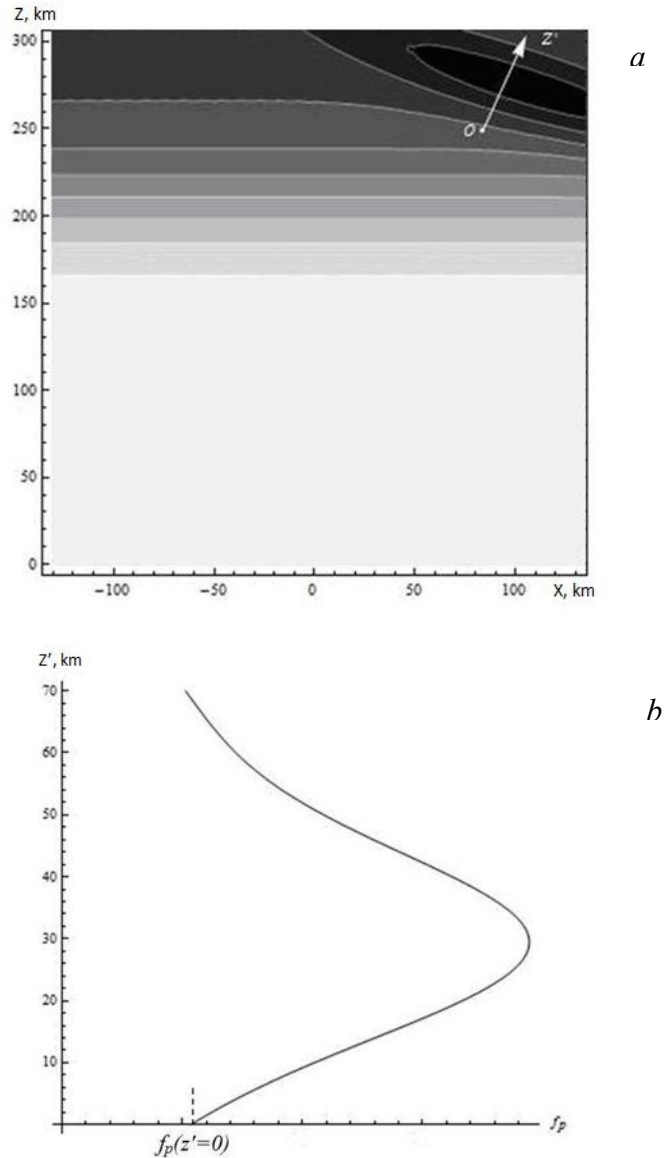


Figure 3. Electron density distribution in the disturbed ionosphere for model (2), the Z' axis is at the angle ψ to the vertical (a); plasma frequency profile along the Z' axis (b)

The peak height of layer (5) z'_m in the $X'OZ'$ coordinate system is displaced by Δz relative to the point (Figure 4, a), therefore Δz is an analog of the scale z_b in (2). It is worth putting the parameter Δz constant so that regardless of the point at which the ray enters the layer, points of the attached tilted layer maximum form a straight line (marked with dots in Figure 4, a) parallel to the disturbance boundary. In other words, we believe that to the ray at a certain operating frequency corresponds the point A at which the ray enters the layer (i.e. at this very point the ray path is normal to the boundary). After the point, the ray propagates in the attached tilted layer of form (5). At another operating frequency, the point B corresponds to the right-angle entry into the disturbance, and the respective tilted layer has another critical frequency f_{c1} and another value of y'_m . Yet the scale Δz remains unchanged so that no reflected rays in the tilted layer can intersect the dotted line in Figure 4, a, whereas, for instance, the ray BQ, which most closely approaches the line, contributes to the right asymptote to cusp. This situation is best illustrated in Figure 3, a, where the perpendicular to the OZ' line, which passes through the center of the disturbance and corresponds to the maximum electron densities, is similar to the dotted line in Figure 4, a.

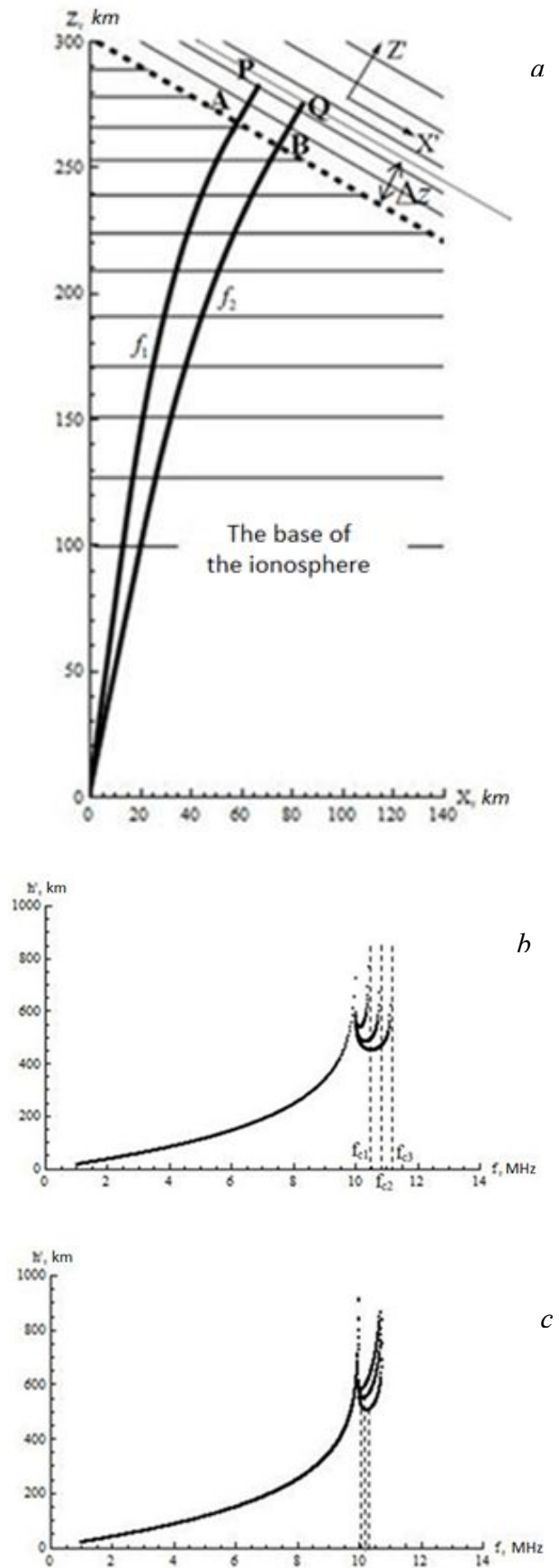


Figure 4. Model of compound parabolic layer (a); variation in perturbation amplitude (b); variation in disturbance scale (c)

From the condition of continuity at the point where layers are smoothly joined, we can easily obtain

$$f_p^2(z_A) = f_p^2(z_A)(1+\delta)^2 \left[1 - \left(\frac{z_A - (z_A + \Delta z)}{y'_m} \right)^2 \right] \text{ and the semi-thickness takes the form } y'_m = \Delta z \frac{1+\delta}{\sqrt{2\delta+\delta^2}}.$$

Note that since the critical frequency f_{c1} in (5) is defined by the perturbation amplitude δ , the width of the cusp in the ionogram monotonously depends on δ . This conclusion is further confirmed by simulation.

Since $f_p(z_A) > f_p(z_B)$, the rays AP and BQ do propagate in different media, i.e., strictly speaking, the tilted layer is not stratified in the X'OZ' coordinate system and the assumption about rectilinear propagation within the layer is only an approximation. Nevertheless, the simulation indicates that this method simulates propagation in model (2) fairly well and hence agrees with the experiment.

The concept of the compound parabolic layer is developed from the idea about tilted ionospheric reflector [Lynn et al., 2013]. However, in its present version the reflector is semitransparent, its reflecting properties depend on the operating frequency so that the rays at the frequencies near f_{c1} gain a great group delay, and at the frequencies above f_{c1} they undergo no reflection. This in particular allows us to describe the formation of the right asymptote to cusp on the ionograms.

DIRECT PROBLEM:

DEPENDENCE OF THE SHAPE OF THE CUSP ON TID PARAMETERS

The simulation shows that the enhancement of perturbation amplitude δ causes the cusp on the ionogram to expand. Figure 4, *b* presents the simulation results for the background layer of type (3) with $f_c=10$ MHz, $z_m=300$ km, $y_m=200$ km (this profile is given in Figure 5, *a*, curve 2), and for tilted layer (5) with $\Delta z=25$ km, the tilt of the boundary line $\psi=30^\circ$, and δ takes on values 6, 10, and 14 %.

In Figure 4, *c*, the parameter Δz assumes values 25, 40, and 55 km at $\delta=10$ %. One can see that the increase in Δz brings about a leftward shift of the bottom of the cusp with its width being constant.

Variations in the tilt of disturbance ψ , as the δ parameter, produce variations in the cusp width. This ambiguity is expected to hinder the solution of the inverse problem of determining TID characteristics from the shape of the cusp – two different parameters give similar patterns of relationship.

Of particular interest is the study of TID temporal evolution, using sequences of experimental ionograms. The descent of the cusp in height in Figure 1 is associated with TID passage; and in the model of compound layer, this in turn corresponds to a shift of the tilted layer in Figure 4, *a*. Assuming that the boundary line shifts parallel to itself ($\psi=const$) and uniformly ($x_0(t)=V_x t$ or $z_0(t)=V_z t$, where $V_z=V_x \text{tg}\psi$), I consider temporal evolution of the synthesized cusp for different cases.

Figure 5, *b* presents four positions of the U-shaped trace for the background profile of type 2 (Figure 5, *a*) and for the attached tilted layer $\Delta z=25$ km, $\delta=10$ %, $\psi=30^\circ$, whereas the parameter z_0 specifying the position of the dashed line in Figure 3, *a* takes on values from 310 to 265 with a step of 15 km, i.e. the step with respect to x is $15/\text{tg}30^\circ=26$ km.

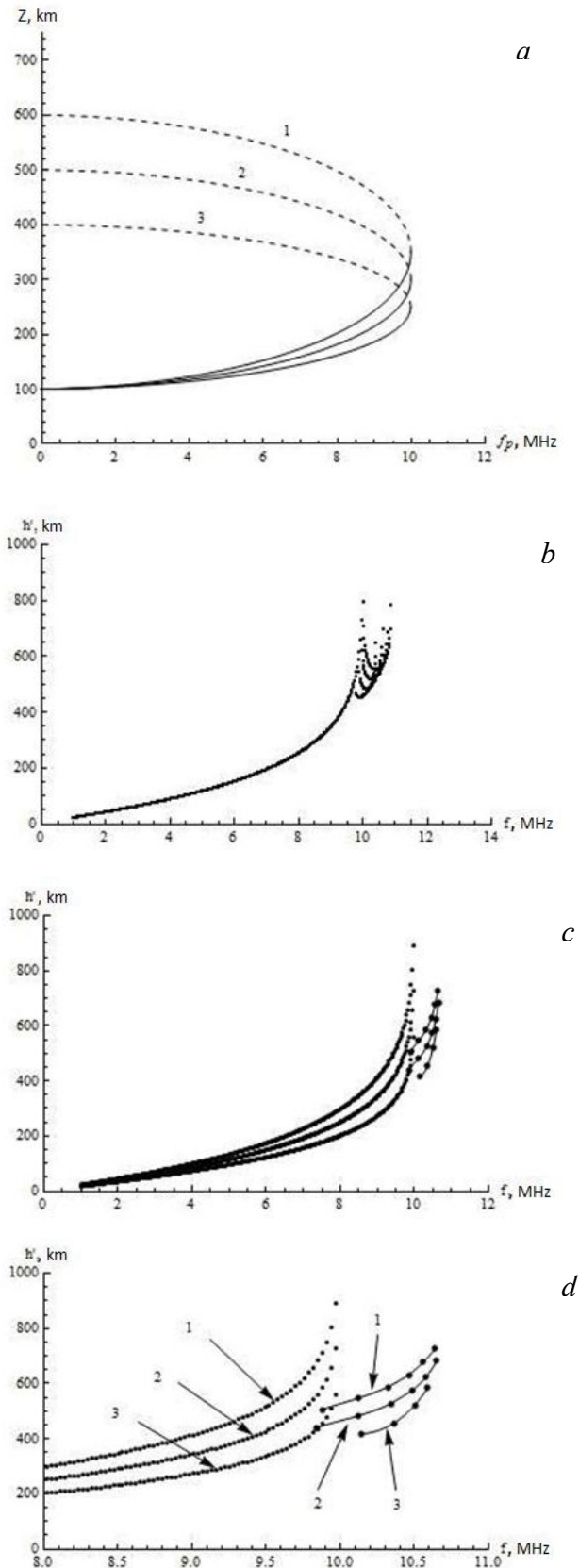


Figure 5. Synthesis of ionograms with U-shaped traces

Let us define the virtual h'f trace of the cusp as the curve which is described by the bottom of the cusp (along h') as it descends. Figure 5, *d* is a magnified version of Figure 5 *c* illustrating the h'f trace of the cusp (as a result of

interpolation) for three types of the background profile (Figure 5, *a*); the correspondence between the profile and the h'f trace is numbered 1, 2, 3. It can be seen that variations in the slope of H'F TRACE associated with variations in the peak height of the background layer lead to respective variations in the slope of h'f trace of the cusp. This appears quite reasonable. It is clear that a rise in the TID velocity causes a rise in the speed of cusp descent along the respective h'f trace.

DISCUSSION

When examining U-shaped traces on the ionograms, it seems reasonable to propose a method enabling us to avoid computational overheads of numerical ray tracing in synthesizing ionograms in the disturbed ionosphere. This may be particularly topical when simulating oblique ionograms with characteristic multipath propagation (so-called Z-shaped signatures in ionograms). In this case, the homing-in procedure implies coverage of a wide range of angles with a very small step. In the proposed method, the necessity for homing-in still remains, but the parabolic approximation of the medium allows us to avoid numerical solution of ray equations.

The simulation shows that the synthesized cusps reproduce experimental data for disturbance amplitudes of about 10 % and scales on the order of tens of kilometers, which exceed the first Fresnel zone. Given these values of the disturbance characteristics, the cusps follow the same pattern as simulated with Gaussian enhancement (for example, broadening of the cusp with increasing amplitude).

Notice that the proposed method allows adequate imitation of U-shaped traces only until they merge with the main trace. The merging can be described by more complicated models, say, the Gaussian enhancement. On the other hand, solving the inverse problem of determining TID characteristics may pose some difficulties for the complicated models. The inverse problem here is solved by varying the disturbance features until the observed cusps are acceptably reproduced. For this reason, the fitting procedure may take inadmissibly long time. This express method can be used as the first approximation to estimate the TID characteristics, switching then to more realistic models of ionospheric disturbances.

CONCLUSION

The described method enables us to avoid computational overheads of numerical ray tracing in synthesizing ionograms under conditions of horizontal electron density gradients. The model of compound parabolic layer has been shown to correlate fairly satisfactorily with those models of nonstratified medium, which in turn adequately describe the disturbed ionograms.

In this context, it seems reasonable to pose an inverse problem of determining parameters of ionospheric disturbances from disturbed ionograms. This however involves some difficulties:

1. It is not always possible to clearly identify U-shaped traces on experimental ionograms, to discern asymptotes and bottom of the cusp.

2. Solving the direct problem shows that variations in two independent disturbance parameters can result in similar changes in a synthesized ionogram.

APPENDIX 1

In the geometrical optics approximation, ray equations may be written as [Kravtsov, Orlov, 1990]

$$\frac{d^2 \vec{r}}{d\tau^2} = \frac{1}{2} \nabla \varepsilon, \quad (1a)$$

where \vec{r} is the radius vector, τ is the group path of wave, $\varepsilon = 1 - \frac{f_p^2}{f^2}$ is the refractive index of medium, f is the operating frequency, f_p is the plasma frequency.

In a two-dimensional case, Expression (1a) is transformed into the system of equations

$$\frac{d^2 x}{d\tau^2} = \frac{1}{2} \frac{\partial \varepsilon}{\partial x}; \quad \frac{d^2 z}{d\tau^2} = \frac{1}{2} \frac{\partial \varepsilon}{\partial z}. \quad (2a)$$

Consider the parabolic layer of the form

$$f_p^2(z) = f_c^2 \left[1 - \left(\frac{z - z_m}{y_m} \right)^2 \right]. \quad (3a)$$

For the stratified medium of type (3a), the permittivity does not depend on the horizontal coordinate, $\partial \varepsilon / \partial x = 0$, and system (2a) takes the form [Eremenko et al., 2007]

$$\frac{d^2 x}{d\tau^2} = 0; \quad \frac{d^2 z}{d\tau^2} = \frac{f_c^2}{f^2} \frac{z - z_m}{y_m^2}. \quad (4a)$$

Suppose that a ray from a transmitter propagates rectilinearly to the base of the ionosphere, and the ray enters the ionospheric layer (the point $z = z_m - y_m$) at the initial angle φ_0 to the horizon at the origin:

$$\begin{aligned} x(\tau = 0) &= z(\tau = 0) = 0; \\ (dx(\tau = 0)) / d\tau &= \cos \varphi_0; \\ (dz(\tau = 0)) / d\tau &= \sin \varphi_0. \end{aligned} \quad (5a)$$

The solution of (4a) takes the form

$$x(\tau) = \cos \varphi_0 \tau, \quad (6a)$$

$$z(\tau) = A_1 e^{\Omega \tau} + A_2 e^{-\Omega \tau} + z_m, \quad (7a)$$

where $\Omega = \frac{f_c}{f} \frac{1}{y_m}$, and the constants A_1 and A_2 are determined from initial conditions (5a):

$$A_{1,2} = \frac{1}{2} \left(\pm \frac{\sin \varphi_0}{\Omega} - z_m \right).$$

For the path, we finally get

$$z(x) = A_1 \exp\left(\frac{\Omega x}{\cos \varphi_0}\right) + A_2 \exp\left(-\frac{\Omega x}{\cos \varphi_0}\right) + z_m. \quad 8a)$$

The group path of wave τ_1 as it propagates in the ionospheric layer is prescribed by $z(\tau_1)=0$: $\tau_1 = \frac{1}{\Omega} \ln \frac{A_2}{A_1}$, and

the increment describing propagation in vacuum before entering the ionosphere is $\tau_0 = \frac{z_m - y_m}{\sin \varphi_0}$.

The author expresses gratitude to A.V. Podlesnyi for providing experimental data.

This study was supported by the Russian Foundation for Basic Research (grant No. 14-05-00259).

REFERENCES

- Danilkin N.P., Lukin D.S., Stasevich V.I. Trajectory synthesis of ionograms in the presence of artificial ionospheric inhomogeneities. *Geomagnetizm i aeronomiya* [Geomagnetism and Aeronomy]. 1987, vol. 27, pp. 217–224. (In Russian).
- Eremenko V.A., Krashennikov I.V., Cherkashin Yu.N. Specific behaviour of the radioemission wave field near the maximum usable frequency. *Geomagnetizm and Aeronomy*. 2007, vol. 47, no. 3, pp. 383–388.
- Krashennikov I.V., Lyannoi B.E. On the interpretation of one type of traveling ionospheric disturbance using vertical incidence ionograms. *Geomagnetizm i aeronomiya* [Geomagnetism and Aeronomy]. 1991, vol. 31, no. 3, pp. 427–433. (In Russian).
- Kravtsov Yu.A., Orlov Yu.I. *Geometrical Optics of Inhomogeneous Media*. Springer-Verlag Publ., 1990, 312 p.
- Laryunin O.A., Kurkin V.I., Podlesnyi A.V. Using two closely-spaced ionosondes in diagnostics of traveling ionospheric disturbances. *Electromagnitnye volny i elektronnye sistemy* [Electromagnetic Waves and Electronic Systems]. 2014, vol. 19, no. 1, pp. 10–17. (In Russian).
- Lynn K.J.W., Otsuka Y., Shiokawa K. Ionogram-based range-time displays for observing relationships between ionosonde satellite traces, spread F and drifting optical plasma depletions. *J. Atm. Solar-Terr. Phys.* 2013, vol. 98, pp. 105–112.
- Munro G.H., Heisler L.H. Cusp type anomalies in variable frequency ionospheric records. *Australian J. Phys.* 1956, vol. 9, pp. 343–357.